2023 Sixth International Symposium on Computer, Consumer and Control (IS3C) | 979-8-3503-0195-3/23/$31.00 ©2023 IEEE | DOI: 10.1109/IS3C57901.2023.00039

A Refractive Distortion Correction Method for 3D Root Reconstruction

Mu-Wei Li
Department of Computer Science and Engineering
National Chung Hsing University
Taichung, 40227, Taiwan, ROC
limuwei1993@gmail.com

Shuen-Fang Lo
Biotechnology Center
National Chung Hsing University
Taichung, 40227, Taiwan, ROC
jjpipilo@gmail.com

Shyr-Shen Yu
Department of Computer Science and Engineering
National Chung Hsing University
Taichung, 40227, Taiwan, ROC
pyu@nchu.edu.tw

Po-Lung Wu
Department of Digital Content Design
Ling Tung University
Taichung, 40852, Taiwan, ROC
wupolung@wustudio.net

Yung-Kuan Chan
Department of Management Information Systems
National Chung Hsing University
Taichung, 40227, Taiwan, ROC
ykchan@nchu.edu.tw

***Abstract* - Measurement of plant root system architecture (RSA) traits is an important task for botany. Usually, the botanists put the plants in a transparent gel container for easy observation. Under this configuration, an easy-to-use way to measure RSA traits is to take images for observation. However, in single-view-angle 2D image often has problems such as occlusion and lack of depth information, so it is not convenient for measurement. Therefore, the reconstruction of the 3D root model from multi-view-angle images is a better solution. Under the above-mentioned planting configuration, the refractive distortion problem usually arises. This will lead to serious distortion of model reconstruction, so in this paper, a method based on ray tracing for correcting refraction distortion of objects in cylindrical containers is proposed.**

Keywords: Root system architecture, 3D root model reconstruction, Refraction distortion.

I. INTRODUCTION

For botanists, measuring the RSA of plants is valuable, it plays an important role in many botany studies. They can obtain some information on various crops by observing their traits (such as length, area, etc.) [1-3]. These traits are often measured manually, often with several problems. For example, it requires additional labor and time to measure that, and more serious is that it is easy to cause plant damage during the measurement process. Therefore, it is necessary to develop a contactless and automatic measurement method. In order to satisfy these two requirements, taking some images of the root and then performing a series of measurements on the 2D image may be one way. However, the 2D image-based method usually exists some problems, such as occlusion, lack of depth information, etc., resulting in an inaccurate measurement. Based on the above-mentioned reasons, the 3D model is the one of most suitable solutions for RSA traits measurement.

To measure RSA traits from a 3D model, there must first be a way to acquire the 3D model. Several existing 3D scanners, such as computed tomography (CT) [4-9], magnetic resonance imaging (MRI) [10-13], laser [14], etc. Although these instruments can be relatively accurate in building 3D models, they exist for several reasons that make them unsuitable for general application. First, these instruments are usually very expensive and increase the barriers to research. Second, the design of these instruments may not be suitable for scanning the gel container, it may be difficult to place, or it may cause the gel to flow out when scanning certain viewing angles. Therefore, a low-cost consideration is to use 2D images to reconstruct 3D models, such as [15-19], which use multi-view images taken by general consumer cameras to reconstruct 3D models. Its basic concept is to take 2D images from different angles and combine them to reconstruct a 3D model [20, 21]. Therefore, this method is low-cost. It just needs a turntable and a camera. The existing methods [15-19], usually require additional settings to deal with refraction distortion. In this paper, we focus on solving this problem.

For refraction distortion correction in [15-18] is to place the gel container in a square water tank. The concept of this method is that they make the angle of incidence equal everywhere in the gel container, and the angle of incidence is 0 degrees from the normal. This makes the angle of refraction also equal to 0 degrees so that there is no refraction distortion. However, this method increases the difficulty of operation. In our approach,

979-8-3503-0195-3/23/$31.00 ©2023 IEEE
DOI 10.1109/IS3C57901.2023.00039

we perform a series of ray tracing calculations for the refraction distortion correction method for visual hull-based 3D reconstruction. In our method, the user can simplify the operation process.

II. Related Works

RootReader3D [15,16] provides a 3D RSA reconstruction system for plants planted in a transparent glass container. This system is based on the visual hull method to reconstruct 3D voxels (take an image every 9 degrees). They also provide several physical assistance methods. The first is to add a square water tank to correct the refraction by placing the container in the water tank. Second, add a calibration rod with the index mask to correct the axis of rotation. After reconstructing the 3D RSA, they also calculated several RSA traits.

Zheng et al. [17] also put the gel container in a square water tank to correct the refraction distortion. After that, they used the hysteresis threshold to segment out the root part from the 2D image. Similar to the above-mentioned research, they also use the concept of the visual hull to reconstruct 3D voxels, in their method, a consistency function is defined, and this function is used to alleviate refraction and jitter distortion. Finally, in order to make the model better connected, they repair the model based on the minimal spanning tree. Subsequently, the system was also applied to record the growth of plants [18].

We can find that the above two systems have a common problem, that is the refraction distortion. Besides their approach as in [15-18] where they place the gel container in a square tank, there is another approach to deal with refractive distortion as in [19], they wash out the roots directly. This approach directly avoids the problem of refraction distortion. One advantage is that they can be grown in other opaque mediums, such as soil, making it easier to grow plants. The above-mentioned two methods including adding a glass water tank and directly washing out the root can make the 2D image directly without distortion. And these two methods have one of the most important shortcomings, both of which make the operation more complicated and require more complicated mechanism design. The latter may even harm the plant. In order to make the operation easier, we can solve the refraction problem from another point of view. In the refraction distortion 2D image, through some ray tracing calculations to get their true position.

III. Method

A. Data acquire

We planted one rice seed in each gel container and photographed it seven days after germination. We shoot an image at an interval of 5 degrees, and each set of data contains a total of 72 images. A sample image of a set is shown in Fig. 1. Then, we segment the foreground from each 2D image, such as the white pixel in Fig. 2, and we perform 3D reconstruction on these foreground pixels.

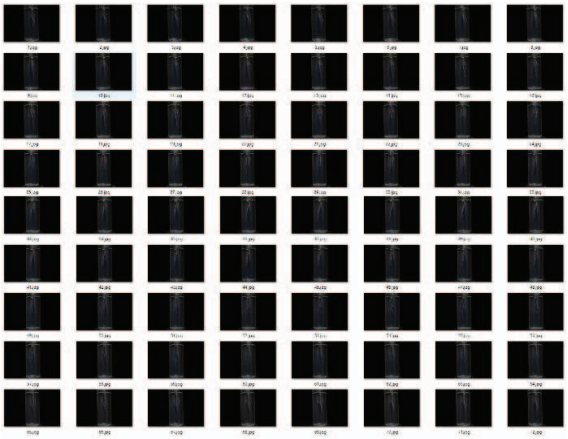

Fig. 1 A set of root images taken from 72 angles.

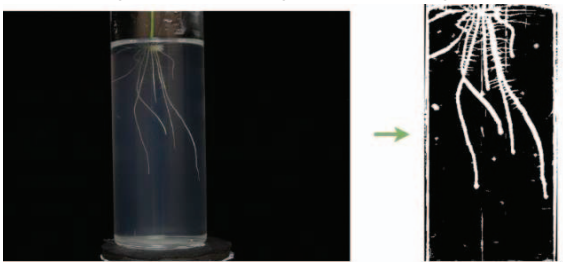

Fig. 2 A example of foreground segmentation.

B. Refractive Distortion Correction

For the gel container, it is a cylinder, the refractive index of the inner and outer media is different, and the difference in the angle of incidence is shown in the Fig. 3. Assuming that an object is imaged at the green point of the camera, its true possible position is all the positions of the corresponding blue dotted line. Therefore, we list the paths passed as candidate points, to do this, we need to do ray tracing for its path. (to illustrate the ray tracing process more clearly, all the symbols of equation (1) to (9) are visible in Fig. 4) First, we define a coordinate transform function as (1):

$$T(x,z) = (x - x'', z), \quad (1)$$

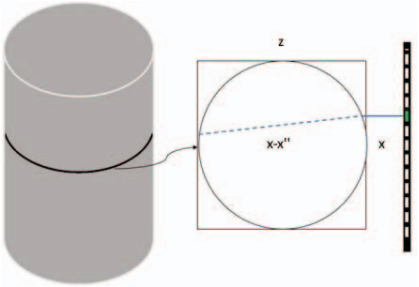

Fig. 3 Refraction distortion at a certain y-axis slice.

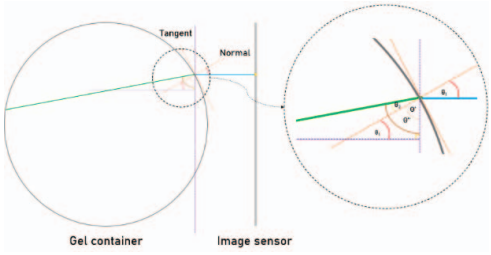

Fig. 4 Refractive distortion correction.

For convenience, we rewrite $x - x''$ as x', the coordinates after transform shown as (2):

$$T(x,z) = (x - x'', z) = (x', z), (2)$$

x' is candidate points at z position, x is the position without refraction distortion, x'' shown as (3):

$$x'' = z * cot(\theta''), (3)$$

Therefore, we have to calculate θ''. And we can divide θ'' into two angles, θ' and θ_2.

$$\theta'' = \theta' + \theta_2, (4)$$

Then, we can use the incident angle θ_1, to get θ', we only need to calculate the angle between the normal on the tangent of the incident light and the camera, which is θ_1, in order to calculate this angle, we form a triangle with the normal, the camera, and the path without refraction, the sum of the three angles of the triangle is π, and the angle between the camera and the path without refraction are $\pi/2$, therefore, θ' is calculated as (5).

$$\theta' = \pi - \frac{\pi}{2} - \theta_1, (5)$$

Next, we use Snell's law to calculate θ_2, Snell's law is defined as (6).

$$(sin\theta_2 / sin\theta_1) = (n_1 / n_2), (6)$$

n_1 and n_2 are indices of refraction inside and outside the gel container media respectively, θ_1 is the angle of incidence, θ_2 is the indices of refraction. n_1 and n_2 are the refractive index of two different media, in our scenario, the ray path is air, then the outer glass of the gel container, and then the inner culture medium of the gel container, the refractive index of air is 1.000277, and in our material, the refractive index of the gel container is 1.474 and 1.333 refractive index for the culture medium. θ_1 can be calculated as (7).

$$\theta_1 = \frac{\left(i(x) - \frac{w}{2}\right)}{w} * \pi, (7)$$

$i(x)$ is width index on image, w is width of image. Therefore, the angle of incidence from left to right is from -90 degrees to 90 degrees, so when object in the middle of the image, the incident angle is 0, it has no distortion. The farther away from the center point, the more serious the distortion. After we know the θ_1, n_1 and n_2, we can calculate θ_2, so we rewrite equation (7) to (8).

$$\theta_2 = arcsin(n_1/n_2) * sin\theta_1, (8)$$

We rewrite the equation (2) using equation (3) to equation (8), and its possible x position at a certain z position is as (9):

$$T(x,z) = (x',z) = \left(x - z * cot\left(\pi - \frac{\pi}{2} - \left(\frac{(i(x) - w/2)}{w}\right) * \pi + arcsin\left(\frac{n_1}{n_2}\right) * sin\theta_1\right), z\right), (9)$$

C. 3D Root Model Reconstruction

In the step of 3D root model reconstruction, we first generate a set of candidate 3D points. Our method is based on the visual hull. Unlike the general approach, we will correct for refraction distortion. When the 2D image is the root part, we emit a ray from this pixel, and the path of this ray is as in equation (9). And according to the taken angle of the image, we rotated the model to the corresponding angle and then projected it. The process of visual hull generation is shown in Fig. 5. On a certain slice (y = a certain value), for the convenience of presentation, the diagram in Fig.5 is emitted from 4 angles (actually we use 72 angles). In the image, the white dots indicate the existence of objects, and the 4 colors indicate the dots generated from the images from 4 different angles. After this step, all possible candidate points have been generated.

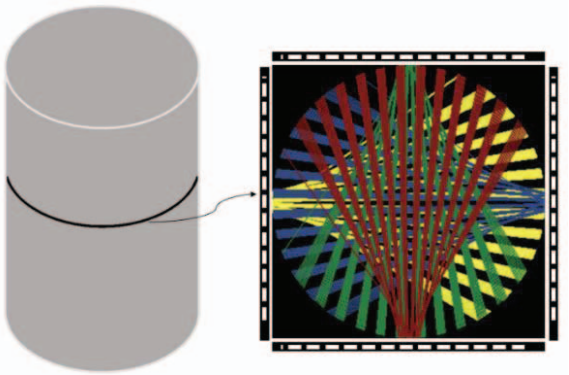

Fig. 5 A Example of 3D candidate point generation.

The candidate points generated from the previous step are much greater than the actual number of points. Because the ray path emitted from one pixel is considered to be a possible real position, it will generate D points in 3D space (D is the depth of the gel container). it may actually have only one point in the three-dimensional space. In order to reduce the number of points, we need to set a threshold value T_c. When the overlap rate of the point in the 3D space is greater than T_c, it will be retained. In this paper, we set T_c. as the median of overlap rates in all 3D spaces.

IV. Experimental

We show several reconstruction results in Fig. 6. From left to right are 0-degree 2D images, and 3D model reconstruction results without/with refraction correction. It can be clearly observed that the 3D model without refraction correction misses many points, which is due to the distortion of refraction, which leads to the incorrect reconstruction of many points due to insufficient overlap.

Fig. 6 Several 3D root model reconstruction examples.

V. Conclusions and Future Works

We propose a refraction correction method for visual hull-based 3D reconstruction of plant roots in gel containers, and the results also show that a more accurate 3D root model can be obtained after its correction.

In future work, for plants in gel containers, 3D root models can be reconstructed based on our refraction correction method, and various RSA traits are estimated for use by botanists. In addition, the reconstruction method provided in this paper still needs to be further improved for lateral roots, in the future it is also an important task.

References

[1] E. D. Rogers and P. N. Benfey, "Regulation of plant root system architecture: implications for crop advancement," Current Opinion in Biotechnology, vol. 32, pp. 93–98, 2015.

[2] M. Saleem, A. D. Law, M. R. Sahib, Z. H. Pervaiz, and Q. Zhang, "Impact of root system architecture on rhizosphere and root microbiome," Rhizosphere, vol. 6, pp. 47–51, 2018.

[3] M. Lombardi, L. De Gara, and F. Loreto, "Determinants of root system architecture for future-ready, stress-resilient crops," Physiologia Plantarum, vol. 172, no. 4, pp. 2090–2097, 2021.

[4] S. Mairhofer, C. J. Sturrock, M. J. Bennett, S. J. Mooney, and T. P. Pridmore, "Extracting multiple interacting root systems using x-ray microcomputed tomography," The Plant Journal, vol. 84, no. 5, pp. 1034–1043, 2015.

[5] S. R. Tracy, C. R. Black, J. A. Roberts, I. C. Dodd, and S. J. Mooney, "Using x-ray computed tomography to explore the role of abscisic acid in moderating the impact of soil compaction on root system architecture," Environmental and Experimental Botany, vol. 110, pp. 11–18, 2015.

[6] S. Ahmed, T. N. Klassen, S. Keyes, M. Daly, D. L. Jones, M. Mavrogordato, I. Sinclair, and T. Roose, "Imaging the interaction of roots and phosphate fertiliser granules using 4d x-ray tomography," Plant and Soil, vol. 401, no. 1, pp. 125– 134, 2016.

[7] L. Popova, D. van Dusschoten, K. A. Nagel, F. Fiorani, and B. Mazzolai, "Plant root tortuosity: an indicator of root path formation in soil with different composition and density," Annals of botany, vol. 118, no. 4, pp. 685–698, 2016.

[8] S. Teramoto, S. Takayasu, Y. Kitomi, Y. Arai-Sanoh, T. Tanabata, and Y. Uga, "High-throughput three-dimensional visualization of root system architecture of rice using x-ray computed tomography," Plant Methods, vol. 16, pp. 1–14, 2020.

[9] P. Xiong, Z. Zhang, P. D. Hallett, and X. Peng, "Variable responses of maize root architecture in elite cultivars due to soil compaction and moisture," Plant and Soil, vol. 455, no. 1, pp. 79–91, 2020.

[10] H. Schulz, J. A. Postma, D. van Dusschoten, H. Scharr, and S. Behnke, "Plant root system analysis from mri images," in Computer Vision, Imaging and Computer Graphics. Theory and Application, pp. 411–425, Springer, 2013.

[11] D. van Dusschoten, R. Metzner, J. Kochs, J. A. Postma, D. Pflugfelder, J. B¨uhler, U. Schurr, and S. Jahnke, "Quantitative 3d analysis of plant roots growing in soil using magnetic resonance imaging," Plant physiology, vol. 170, no. 3, pp. 1176–1188, 2016.

[12] K. Yoshino, Y. Numajiri, S. Teramoto, N. Kawachi, T. Tanabata, T. Tanaka, T. Hayashi, T. Kawakatsu, and Y. Uga, "Towards a deeper integrated multi-omics approach in the root system to develop climate-resilient rice," Molecular Breeding, vol. 39, no. 12, pp. 1–19, 2019.

[13] S. Teramoto, T. Tanabata, and Y. Uga, "Rsatrace3d: robust vectorization software for measuring monocot root system architecture," BMC Plant Biology, vol. 21, no. 1, pp. 1–11, 2021.

[14] S. Fang, X. Yan, and H. Liao, "3d reconstruction and dynamic modeling of root architecture in situ and its application to crop phosphorus research," The Plant Journal, vol. 60, no. 6, pp. 1096–1108, 2009.

[15] R. T. Clark, R. B. MacCurdy, J. K. Jung, J. E. Shaff, S. R. McCouch, D. J. Aneshansley, and L. V. Kochian, "Three-dimensional root phenotyping with a novel imaging and software platform," Plant physiology, vol. 156, no. 2, pp. 455–465, 2011. 2

[16] M. A. Pi˜neros, B. G. Larson, J. E. Shaff, D. J. Schneider, A. X. Falc˜ao, L. Yuan, R. T. Clark, E. J. Craft, T. W. Davis, P.-L. Pradier, et al., "Evolving technologies for growing, imaging and analyzing 3d root system architecture of crop plants," Journal of integrative plant biology, vol. 58, no. 3, pp. 230–241, 2016.

[17] Y. Zheng, S. Gu, H. Edelsbrunner, C. Tomasi, and P. Benfey, "Detailed reconstruction of 3d plant root shape," in 2011 International Conference on Computer Vision, pp. 2026–2033, IEEE, 2011.

[18] Symonova, C. N. Topp, and H. Edelsbrunner, "Dynamicroots: a software platform for the reconstruction and analysis of growing plant roots," PLoS One, vol. 10, no. 6, p. e0127657, 2015.

[19] T. Zhu, S. Fang, Z. Li, Y. Liu, H. Liao, and X. Yan, "Quantitative analysis of 3-dimensional root architecture based on image reconstruction and its application to research on phosphorus uptake in soybean," Chinese Science Bulletin, vol. 51, no. 19, pp. 2351–2361, 2006.

[20] Laurentini, "The visual hull concept for silhouette-based image understanding," IEEE Transactions on pattern analysis and machine intelligence, vol. 16, no. 2, pp. 150–162, 1994.

[21] Y. Mulayim, U. Yilmaz, and V. Atalay, "Silhouette-based 3-d model reconstruction from multiple images," IEEE Transactions on Systems, Man, and Cybernetics, Part B (Cybernetics), vol. 33, no. 4, pp. 582–591, 2003.